Experimental evidence for electric surface resistance in niobium

T. Junginger,[1,2,a)] W. Weingarten,[1] and C. P. Welsch[3]
[1)] *CERN, Geneva, Switzerland*
[2)] *MPIK Heidelberg, Germany*
[3)] *Cockcroft Institute, Warrington and University of Liverpool, United Kingdom*

Identifying the loss mechanisms of niobium cavities enables an accurate determination of applications for future accelerator projects and points to research topics required to mitigate current limitations. For several cavities an increasing surface resistance above a threshold field, saturating at higher field has been observed. Measurements on samples give evidence that this effect is caused by the surface electric field. The measured temperature and frequency dependence is consistent with a model that accounts for these losses by interface tunnel exchange between localized states in dielectric oxides and the adjacent superconductor.

PACS numbers: 74.25.nn, 74.78.-w, 74.81.Bd

Superconducting cavities made of niobium are nowadays routinely reaching surface resistances R_S as low as a few nΩ at surface magnetic fields above 100 mT corresponding to peak electric fields of over 50 MV/m, some performing close to the theoretical limit of the material[1]. Nevertheless many open questions concerning the field dependence of R_S exist. Especially in the medium field region between a few and about 100 mT differently prepared cavities show different field dependencies. Some cavities exhibit an increasing, some a decreasing surface resistance. Especially cavities prepared by coating a micrometer thick niobium film on a copper substrate exhibit a strong increase of R_S with field. This paper focuses on cavities which show an increasing R_S with field. For some of these cavities this increase can be fitted with a polynomial of second order. These losses are described by models based on the surface magnetic field $\vec{B}$. Magnetic flux entry is thought to give rise to the quadratic term, which is dependent on temperature[2], while the linear term is correlated to hysteresis losses and independent of temperature[3]. Adding an additional term to account for a widely observed decrease of R_S at fields below a few mT[2] the total surface resistance for a cavity measured at a fixed temperature can be written as:

$$R_S = R_0 + R_1\left(\frac{B}{B_c}\right) + R_2\left(\frac{B}{B_c}\right)^2 + R_3\left(\frac{1}{B}\right)^2, \quad (1)$$

where the critical thermodynamic field B_c is 200 mT for niobium[4]. Even if these losses constitute the major contribution for most cavities, it is important to identify other loss types in order to disentangle them correctly. In this spirit we present a different loss mechanism of electrical origin, already observed, though not further quantified, in prototypes of superconducting bulk niobium cavities for the Large Electron Positron Collider at CERN[5]. These losses yield an R_S increasing above a threshold field saturating at higher field[6] and can be explained by the interface tunnel exchange model (ITE)[7].

[a)] New institute: Triumf, Vancouver, BC, Canada, Electronic mail: tobi@triumf.ca

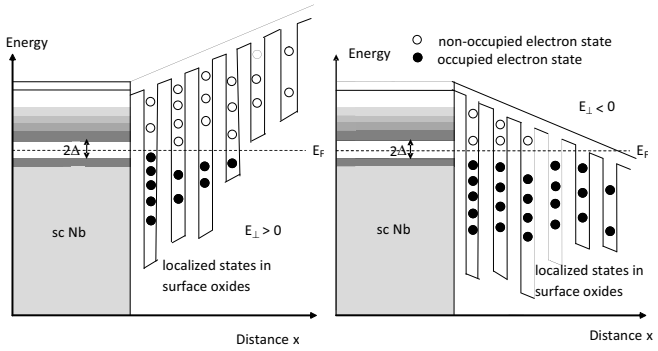

FIG. 1. Schematic view of energy states at thermal equilibrium near the interface of superconducting niobium and dielectric surface oxides; (left) after exposure to a positive and (right) to a negative electric field $E_\perp$. Note that the population of occupied electron states in the oxide is modified after the exposure of the electric field which indicates current flow. In the superconducting niobium (sc Nb) the gray-scales indicate the density of states. E_F is the Fermi energy and Δ is the energy gap of superconducting niobium.

ITE assumes that electrons are exchanged between states in the superconducting Nb and localized states in adjacent dielectric oxides (Nb_2O_5 and/or NbO_2). This exchange is caused by the surface electric field $\vec{E}$ penetrating only the oxide and not the superconductor, allowing for an exchange of electrons (i.e. a current) between the two materials within one RF period. Fig. 1 depicts the variation of the density of occupied electron states before and after an exposure of the surface to a stepwise increase or decrease of the electric field. The time after exposure is considered here long as compared to the relaxation time. Hence the occupation of states is in thermal equilibrium. However, for sufficiently shorter times as in the case of a time-varying RF field the electron current density $\vec{j}$ is not in quadrature with the electric field, which gives rise to RF losses $\vec{j}\cdot\vec{E}$, and hence to an electric surface resistance R_S^E. As the electrons relax and dissipate once per RF period R_S^E depends linearly on the RF frequency f. Within the superconducting energy gap 2Δ there are no electronic states available for a current to flow. There-

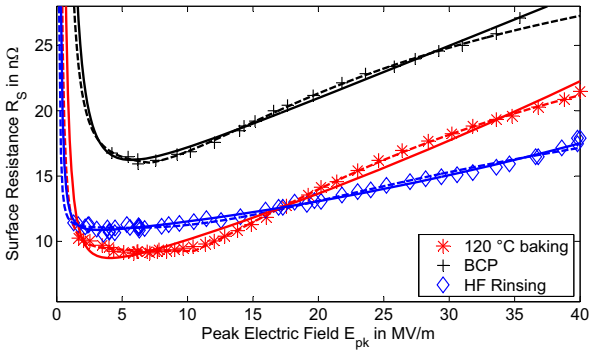

FIG. 2. Surface resistance of an elliptical 1300 MHz bulk niobium cavity at 2 K. The dashed lines show fits to the ITE model (Eq. 5 while the solid lines show fits to Eq. 1. Data taken by Romanenko et al.[8]

fore there exists a threshold electric field E^0, depending on the thickness of the oxide x and on Δ, below which there is no current and hence no RF loss. In a quantitative analysis, Halbritter calculated the surface resistance for ITE losses as[7]:

$$R_S^E = R_{S,sat}^E f[\mathrm{GHz}] \left[e^{-b/E} - e^{-b/E^0} \right], \quad E \geq E^0, \quad (2)$$

where the parameters R_S^E (here normalized to 1 GHz) , b and E^0 are defined by

$$b = \frac{2\kappa\Delta\varepsilon_r}{\beta^* e}, \quad R_{S,sat}^E = \frac{2\pi\mu_0}{(2\kappa)^2 y}, \quad E^0 = \frac{\Delta\varepsilon_r}{ex\beta^*} \quad (3)$$

with

$$\kappa = \sqrt{2m\,(E_c - E_F)}/\hbar, \quad y^{-1} = \frac{\langle x n_T \rangle\, e^2}{\varepsilon_0 \varepsilon_r}. \quad (4)$$

The meaning of the physical parameters is the following: E_c and E_F are the energies of the conduction band and the Fermi energy, respectively; $\langle x n_T \rangle$ is the averaged product of the density of trapped electron states n_T and the thickness of the oxide x; ε_r is the relative dielectric constant; β^* is the geometric field enhancement factor of the metal due to surface roughness; m, e, ε_0, μ_0 and $\hbar$ are the usual physical constants, such as the electron mass and electric charge, vacuum permittivity, vacuum permeability and Planck constant, in this order.

Figure 2 shows R_S as a function of the peak electric field E_{pk} at 2 K of a 1.3 GHz elliptical TESLA shaped[9] cavity. It was manufactured of fine grain bulk niobium (grain size of about 50 µm). The first measurement was performed after chemical polishing (BCP). Afterwards the cavity was in situ baked at 120 °C. Then several hydrofluoric (HF) rinsings were done to remove about 10 nm of the outer surface layer[8]. The dashed lines show fits to the ITE model with two additional parameters accounting for the low field losses. The total R_S is assumed to be

$$R_S = R_S^E(E) + R_0 + R_3 \left(\frac{1}{B}\right)^2 \quad (5)$$

where $R_S^E(E)$ is calculated according to Eq. 2. For comparison the data has also been fitted to Eq. 1. Note that the fit to Eq. 1 systematically overestimates the data in the low and high field region, while it systematically underestimates the data in the medium field region for the data obtained after baking (red curve). The measurement is not well represented by the fit even if a relative high coefficient of determination R^2 is obtained. The ITE model however can explain the dependence of R_S on E_{pk} better and significantly higher R^2 values are found for these fits obtained for the two data sets before HF rinsing, see Tab. I. The phenomenological fit parameters (also found in Tab. I) correspond to physical meaningful parameters (compare with[10] and quotations therein and[11,12]) as β^*=1, ε_r=10, $E_c - E_F$=0.05 eV, Δ=1.18 meV, x=1.65 nm and $\langle n_T \rangle$=3.1·10^{24} 1/(eVm^3), before and β^*=1, ε_r=10, $E_c - E_F$=0.05 eV, Δ=1.33 meV, x=1.27 nm and $\langle n_T \rangle$=4.9·10^{24} 1/(eVm^3) after baking. The values of $E_c - E_F$ are inconsistent with the band gap of Nb_2O_2 (3.4-5.3 eV[13]) but fit neatly the value of NbO_2 (0.1 eV[14]). Hence the localized states participating in the exchange are found the NbO_2 for which the value of ε_r=10 is consistent with[15]. Recent results show that after mild baking the total thickness of the oxide layer is reduced, but the thickness of the NbO_2 layer enhanced[11], which is consistent with an enhanced $R_{S,sat}^E$ and corresponding $\langle n_T \rangle$. After HF rinsing the threshold disappears and the polynomial fit yields a better representation of the data. ITE losses require localized states inside a sufficiently thick dielectric (in this case NbO_2). Vanishing ITE after HF rinsing might be explained by a regrowth of a thinner fresh oxide layer with reduced NbO_2 content.

A cavity test performed at fixed temperature and frequency is obviously not suited to test how the losses depend on these two external parameters. The Quadrupole Resonator[16] is a unique device enabling to test R_S of superconducting samples over a wide parameter range. It features two excitable modes at 400 and 800 MHz with identical magnetic field configuration on the sample

TABLE I. Parameters derived for a least squares fit to Eq. 5 and 1 of a bulk niobium cavity (cf. Fig. 2).

	BCP	120 °C baking	HF rinsing
$R_{S,sat}^E$ in nΩ	18.4±0.8	22.3±0.9	14.0±1.4
E^0 in MV/m	7.1±1.2	10.5±0.5	4±250 [a]
b in MV/m	26.9±1.2	30±3	44±4
R_0 in nΩ	16.6±0.4	9.24±0.09	11.0±0.2
R_3 in nΩ(mT)^2	100±50	15±3	3±3
R^2 for Eq. 5	0.9987	0.9988	0.9885
R_0 in nΩ	12.8±0.5	6.9±0.8	10.4±0.2
R_1 in nΩ	38±2	27±8	6.5±1.9
R_2 in nΩ	0	20±6	19±4
R_3 in nΩ(mT)^2	170±80	48±16	9±3
R^2 for Eq. 1	0.9913	0.9821	0.9926

[a] The threshold effect disappeared for this data set. The ITE model is not applicable here

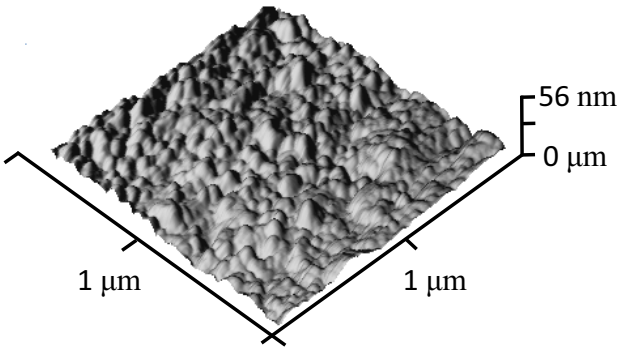

FIG. 3. Surface profile from the niobium film sample obtained from AFM. The lateral resolution of the image is 4 nm.

surface. The ratio between electric and magnetic field for these two modes is proportional to f. For example for a peak magnetic field B_p=10 mT, the peak electric fields are E_p=0.52 and 1.04 MV/m for 400 and 800 MHz, respectively[17]. This feature allows for a separation of magnetic and electrical losses from measurement data by comparison with theoretical models.

To test the properties of ITE a sample is required for which these temperature independent losses remain dominant up to relatively large temperatures. This condition was obtained for a micrometer thin niobium film sample sputtered on a copper substrate, which was kept under normal air for 10 years. Using XPS the thickness of its surface layer was found be significantly larger as a reference bulk niobium sample prepared by BCP[6]. The thin film has a grain size of a few nm as measured by atomic force microscopy, see Fig 3. This is several orders of magnitude smaller than typical values of fine grain bulk niobium surfaces prepared for accelerating cavities.

Using the Quadrupole Resonator it was measured at 400 and 800 MHz over a temperature range between 2 and 4.5 K. Figure 4 shows R_S vs. the peak magnetic field B_pk on the sample. Only about one fifth of the data is plotted. To calculate R_S, the measured dissipated RF power on the sample surface P_RF, is assumed as solely caused by the surface magnetic field using

$$R_\mathrm{S} = \frac{2\mu_0^2 P_\mathrm{RF}}{\int\limits_{\mathrm{Sample}} |\vec{B}|^2 \mathrm{d}S}. \qquad (6)$$

Curves for a different temperature and the same frequency are parallel. Therefore the field dependent part of R_S can be assumed as independent of temperature. Between 0 and 35 mT R_S increases by about 60 nΩ at 400 MHz and by about 600 nΩ at 800 MHz. These two features cannot be explained by any model predicting a linear or quadratic increase of the surface resistance with magnetic field, such as[2,3,18]. In the following it is assumed that the field dependent contribution of R_S is caused by the surface electric field to test whether the data is consistent with the ITE model. First, the field

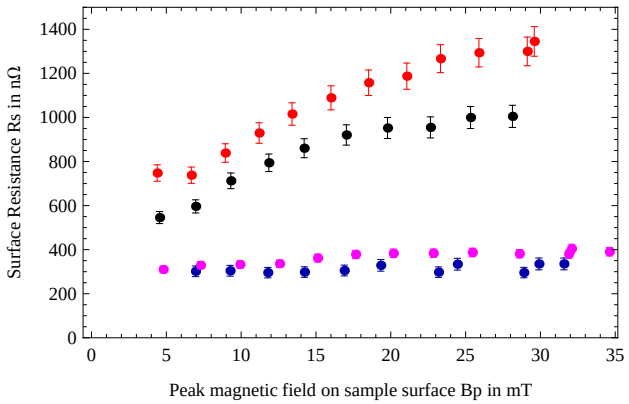

FIG. 4. Surface resistance R_S of a niobium film sample tested with Quadrupole Resonator at 400 MHz (2.5 K (blue), 4 K (magenta)) and 800 MHz (2.5 K (black), 4 K (red). R_S was obtained under the assumption that all losses are solely caused by the surface magnetic field.

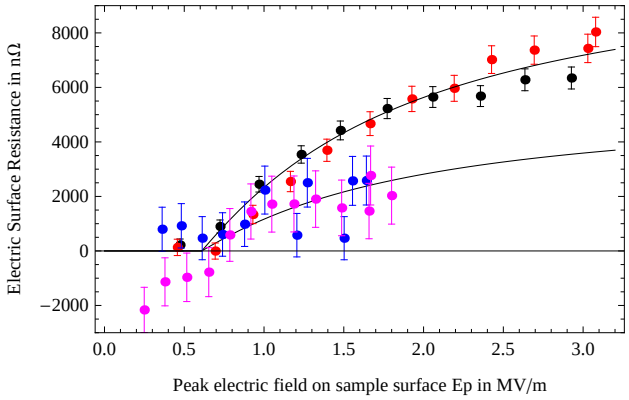

FIG. 5. Electric surface resistance at 400 MHz (2.5 K (blue), 4 K (magenta)) and 800 MHz (2.5 K (black), 4 K (red)) of a niobium film sample. The lines show predictions from a collective least squares multiparameter fit to a data set comprising 183 values $R_\mathrm{S}(f,T,E)$. The data displayed is the same as in Fig. 4. The losses independent on field strength have been subtracted from each curve. All field dependent losses are assumed to be caused by the surface electric field.

independent residual and BCS losses are subtracted from each curve individually. Then R_S is derived assuming all other losses to be caused by the surface electric field using

$$R_\mathrm{S}^\mathrm{E} = \frac{2\mu_0 P_\mathrm{RF}}{\varepsilon_0 \int\limits_{\mathrm{Sample}} |\vec{E}|^2 \mathrm{d}S}. \qquad (7)$$

From Fig. 5 the linear scaling of R_S^E with frequency as predicted by the ITE model becomes apparent. It furthermore becomes more evident that these field dependent losses are independent on temperature. Note that due to the field configuration of the Quadrupole Res-

onator the ratio

$$\int_{\text{Sample}} |\vec{E}|^2 \mathrm{d}S / \int_{\text{Sample}} |\vec{B}|^2 \mathrm{d}S \propto f^2. \quad (8)$$

The complete data set consisting of 183 values $R_S(f,T,E)$ has been collectively fitted to Eq. 2. A χ^2=167.9 was obtained for the fit parameter values of $R^E_{S,sat}$=17000±500 nΩ, b=1.06±0.10 MV/m and E^0=0.610±0.015 MV/m. The value of χ^2 is slightly lower than the number of data points indicating that the experimental uncertainty was a bit overestimated. For this sample $R^E_{S,Sat}$ is three orders of magnitude larger than for the bulk niobium cavity, corresponding to higher density of trapped states. The onset field E^0 is one order of magnitude smaller for the sample, which might be correlated to the roughness of the sample in the nanometer scale, as measured by AFM, see Fig 3. For further surface analytic measurements on this sample in comparison to bulk niobium surfaces refer to[6].

Also here, the phenomenological fit parameters $R^E_{S,sat}$, b and E^0 can be correlated to a set of physical parameters with meaningful values as β^*=10, ε_r=10, $E_c - E_F$=0.01 eV, Δ=1.04 meV, x=1.7 nm and $\langle n_T \rangle$=7·10^{26} 1/(eVm^3). A critical assessment of these numbers lies however beyond the scope of this paper.

In conclusion, the dependency of the surface resistance on the applied field strength is different for different cavities and/or surface preparations. This indicates a variety of different dominant field dependent loss mechanisms. Some cavities exhibit an R_S increasing above a threshold field saturating at higher field. In this paper it has been shown that measurements on a state of the art bulk niobium cavity, showing this behavior of R_S on the surface electric field, can be well described by the ITE model. To further test the predictions of the ITE model a niobium thin film sample was tested with the Quadrupole Resonator. These measurements showed field dependent losses independent on temperature, which scale linearly with frequency, if one assumes that they are caused by the surface electric field. These findings are consistent with the predictions of the ITE model. They allow to better understand the field dependent surface resistance of superconducting niobium. This can be used for the development of future accelerating cavities. In particular a possible explanation for the larger field dependent surface resistance found in some cavities produced of niobium films on copper substrates, a technology widely used for cavity operation at 4.2 K[19], is given by the ITE model.

This work was supported by the German Doctoral Students program of the Federal Ministry of Education and Research (BMBF).

[1] H. Padamsee, *RF superconductivity: Science, Technology, and Applications* (Wiley, New York, NY, 2009).
[2] W. Weingarten, Phys. Rev. ST Accel. Beams **14**, 101002 (2011).
[3] G. Ciovati and J. Halbritter, Physica C **441**, 57 (2006).
[4] H. A. Leupold and H. A. Boorse, Phys. Rev. **134**, 1322 (1964).
[5] P. Bernard et al., Nuclear Instruments & Methods **190**, 257 (1981).
[6] T. Junginger, Ph.D. thesis, University of Heidelberg (2012).
[7] J. Halbritter, Zeitschrift für Physik B **31**, 19 (1978).
[8] A. Romanenko, A. Grassellino, F. Barkov, and J. P. Ozelis, Phys. Rev. ST Accel. Beams **16**, 012001 (2013).
[9] B. Aune et al., Phys. Rev. ST Accel. Beams **3**, 092001 (2000).
[10] J. Halbritter, Applied Physics A - Solids and Surfaces **43**, 1 (1987).
[11] M. Delheusy et al., Appl. Phys. Lett. **92**, 101911 (2008).
[12] Y. Kim, R. Tao, R.F. Klie, and D. N. Seidman, ACSNano **1**, 732 (2013).
[13] J.W. Schultze and M.M Lohrengel, Electrochim Acta **45**, 2499 (2000).
[14] V. Eyert, Europhys. Lett. **58**, 851 (2002).
[15] Y. Zhao, Z. Zhang, and Y. Lin, J. Phys. D: Appl. Phys. **37**, 3392 (2004).
[16] E. Mahner, S. Calatroni, E. Chiaveri, E. Haebel, and J. M. Tessier, Review of Scientific Instruments **74**, 3390 (2003).
[17] T. Junginger, W. Weingarten, and C.P. Welsch, Review of Scientific Instruments **83**, 063902 (2012).
[18] A. Gurevich, Physica C **441**, 38 (2006).
[19] S. Calatroni, Physica C **441**, 95 (2006).